Tolerance of Base Pair Size and Shape in Postlesion DNA Synthesis

Hailey L. Gahlon,[†] W. Bernd Schweizer,[‡] and Shana J. Sturla*[,†]

[†]Department of Health Sciences and Technology, Institute of Food Nutrition and Health, ETH Zürich, Schmelzbergstrasse 9, 8092 Zürich, Switzerland

[‡]Laboratory for Organic Chemistry, D-CHAB, ETH Zürich, Wolfgang-Pauli-Strasse 10, 8093 Zürich, Switzerland

Ⓢ *Supporting Information*

ABSTRACT: The influence of base pair size and shape on the fidelity of DNA polymerase-mediated extension past lesion-containing mispairs was examined. Primer extension analysis was performed with synthetic nucleosides paired opposite the pro-mutagenic DNA lesion O^6-benzylguanine (O^6-BnG). These data indicate that the error-prone DNA polymerase IV (Dpo4) inefficiently extended past the larger Peri:O^6-BnG base pair, and in contrast, error-free extension was observed for the smaller BIM:O^6-BnG base pair. Steady-state kinetic analysis revealed that Dpo4 catalytic efficiency was strongly influenced by the primer:template base pair. Compared to the C:G pair, a 1.9- and 79 000-fold reduction in Dpo4 efficiency was observed for terminal C:O^6-BnG and BIM:G base pairs respectively. These results demonstrate the impact of geometrical size and shape on polymerase-mediated mispair extension.

Figure 1. Structures and DNA sequences used in this study. (a) Wobble base pair between O^6-BnG and C in the active site of Dpo4 (b) synthetic base-modified BIM (1) and Peri (2) and (c) biochemical scheme of Dpo4-mediated primer extension assay.

DNA polymerase enzymes are responsible for gene replication; dysfunctions during DNA synthesis can result in mutations that may lead to cancer. Bulky DNA lesions, resulting from exposure to genotoxic agents (e.g., polycyclic aromatic chemicals, nitrosamines, epoxides) can impede replication and transcription processes.[1,2] Specialized DNA polymerases (i.e., Y-family, e.g. DNA polymerase IV, Dpo4) are devoted to processing these bulky lesions that may otherwise impede DNA replication.[3] Important aspects of error-prone DNA replication include binding of a Y-family polymerase to primer:template DNA, dNTP selection, phosphodiester bond formation, pyrophosphate release, translocation to the subsequent templating base, and potentially repeating the selection and bond-forming process.[4] Y-family polymerases are poorly processive compared to high-fidelity polymerases (e.g., *Thermus aquaticus* DNA polymerase processivity is 50−80 nucleotides per binding event at 55 °C).[5] Dpo4 will dissociate from primer:template DNA after ∼16 dNTP incorporation events (at 37 °C),[6] and these extension steps (i.e., immediately following the lesion) are potentially mutagenic.

The process of postlesion DNA synthesis (PLS) has received little attention despite relevance to DNA damage tolerance. PLS is the extension process immediately following dNTP insertion opposite a DNA adduct (see Figure 1c) and may account for relevant mutations. Studies investigating the ability of Dpo4 to extend past canonical mispairs observed that a G:T mismatch was inefficient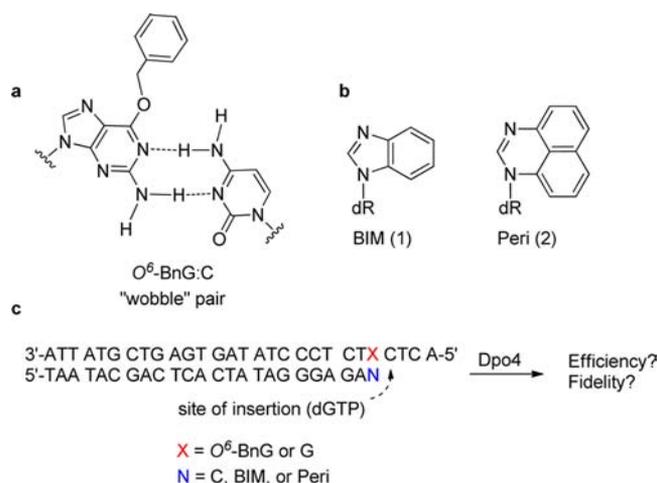ly extended by Dpo4.[7] Crystallographic analysis revealed that the G:T pair contained a reverse wobble that misaligns the 3′-hydroxyl necessary for primer extension.

Much of our current understanding regarding chemical details of polymerase-mediated DNA replication has been gained by studies utilizing non-natural nucleosides as chemical probes.[8−10] A study investigating minor-groove interactions with a deoxyadenosine isostere indicated that mispair extension is dependent on formation of a hydrogen bond between the enzyme (Klenow DNA polymerase) and N3 of the base on the primer oligonucleotide.[11] These studies suggested that base pair geometry may be more important for primer extension vs insertion. The above studies do not address mispair extension with physiological DNA adducts, i.e., PLS. The goal of the present study was to investigate chemical features, i.e., base pair size and shape, which can impact PLS. The strategy involves probing PLS with synthetic nucleosides paired opposite the DNA adduct O^6-BnG. To our knowledge this is the first direct probe to test the influence of base pair size and shape of PLS on O^6-alkylguanine containing templates.

Bulky O^6-alkylguanine DNA adducts, like O^6-BnG, are informative models for investigating DNA polymerase mechanisms and nitrosamine carcinogenesis.[12,13] N-Methylbenzyl-nitrosamine can form O^6-alkylguanine adducts that, if not

repaired, can generate G to A transition mutations during DNA replication.[14] O^6-BnG is bypassed by Dpo4 (dCTP insertion is the major product, approximately 70%).[15] And crystal structures containing a C:O^6-BnG (primer:template) terminal base pair within the active site of Dpo4 reveal a wobble base pair interaction (Figure 1a).[15] Thus, insertion opposite O^6-BnG has been investigated, but PLS remains to be explored.

To our knowledge, there is no information regarding chemical requirements for O^6-alkylguanine PLS. A recent report concerning Dpo4 conformation dynamics during synthesis past 8-oxoG found translocation was inhibited during PLS, suggesting that the inhibition in DNA translocation may facilitate polymerase switching between low- and high-fidelity polymerases.[16] A similar result has been observed in a study regarding pol eta bypass of a TT dimer. Here pol eta observed a higher error rate and lower fidelity while bypassing the 3′ thymine of the dimer in comparison to the 5′ dimer, suggesting that during lesion translocation pol eta can sense differences in dimer location that may be responsible for inducing polymerase switching during lesion bypass.[17]

Previously, we reported an adduct-specific synthetic nucleoside that forms stable DNA duplexes when paired opposite O^6-BnG vs the natural DNA bases.[18] However, no information is available concerning how this or analogous probes behave during polymerase-catalyzed mispair extension. The experimental approach of this study involves evaluating two site-specifically modified oligonucleotides that position the adduct-directed nucleoside probes at the 3′ terminal position of the primer (Figure 1). BIM (1) and Peri (2) contain nucleobase modifications that promote adduct:probe pairing in a DNA duplex. Each structure contains a similar imidazole moiety along the Watson−Crick hydrogen-bonding face, but BIM and Peri differ in size as the result of having one (BIM) or two (Peri) aromatic rings (Figure 1b). Phosphoramidites of BIM and Peri were synthesized for chemical incorporation into oligonucleotides. Crystal structures of BIM and Peri 2′-deoxynucleosides were obtained to confirm relative stereochemistry (Figures S3 and S4). Mutagenesis studies were completed to elucidate the efficiency and fidelity on PLS using the base-modified primers containing BIM and Peri (Figure 1c). Single nucleotide insertion and full length extension studies were performed to assess the ability of Dpo4 to perform PLS on damaged (O^6-BnG) and primer extension on nondamaged (G) templates (Figure 2). Two conditions were investigated for primer extension assays with Dpo4, DNA, and dNTPs: (1) 20 nM, 10 nM, and 100 μM, respectively (Figure 2) and (2) 5 nM, 10 nM, and 50 μM, respectively (Figure S9).

Dpo4-mediated primer extension studies involving the natural 24mer primer revealed reduced fidelity for the G-containing template vs the O^6-BnG-containing template (Figure 2a). Extension of a primer involving a canonical C:G pair at the primer:template terminus (denoted throughout this text as the first base, here C, originating from the primer strand and the second base, here G, from the template strand) revealed low fidelity, and in some cases (dGTP and dATP insertion) multiple incorporations were observed. In the case of dATP insertion, a prominent $n + 2$ extension product band was present due to the template sequence; where T is the $n + 2$ templating base. Additionally, prominent dGTP $n + 2$ bands were observed for the C:G and C:O^6-BnG pairs (albeit lower for C:O^6-BnG, Figure 2). This result was not unexpected since enzyme concentrations were in excess to DNA. However, to test this further, lower enzyme and dNTP concentrations were
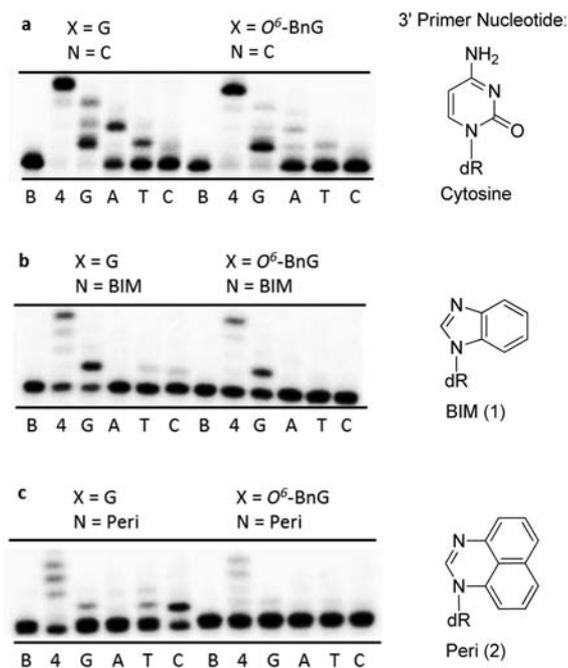

Figure 2. Analysis of Dpo4-mediated primer extension. (B, blank; 4, all four dNTPs; G, dGTP; A, dATP; T, dTTP; C, dCTP). (a) Extension of a natural 24mer primer (see Figure 1c for DNA sequences) opposite G or O^6-BnG. (b) Extension of 24mer 3′-modified BIM primer opposite G or O^6-BnG. (c) Extension of 24mer 3′-modified Peri primer opposite G or O^6-BnG.

investigated. This resulted in decreased $n + 2$ band intensity for both C:G and C:O^6-BnG pairs (Figure S9). Full-length primer extension was highly efficient for C:G and C:O^6-BnG pairs (100% extension products). PLS on the C:O^6-BnG pair revealed high selectivity for products of correct extension (dGTP insertion), with trace amounts of dATP and dTTP extension. With lower enzyme (5 nM) and dNTP (50 μM) concentrations, relative to DNA (10 nM), the correct insertion of dGTP was observed for both G and O^6-BnG templates, and these results revealed a less mutagenic profile (Figure S9) in comparison to higher enzyme and dNTP concentrations. It seems that Dpo4, as a translesion DNA polymerase, is well suited for lesion processing even when the lesion is in the $n − 1$ position (i.e., PLS).

Extension with BIM:G and BIM:O^6-BnG pairs was selective (i.e., only dGTP insertion). A higher percentage of full-length extension was observed for the nondamaged (56%) vs damaged O^6-BnG template (37%), suggesting that the size of a terminal BIM:G base pair is more suited for efficient catalysis to occur in comparison to the BIM:O^6-BnG pair. Lower mutagenicity was observed with the BIM:G pair in comparison to both the C:G and Peri:G pairs. Dpo4-mediated extension with the Peri:G terminal pair contains low levels of dGTP or dTTP extension products (approximately 10% each) and high levels of dCTP extension products (50%). The high amount of dCTP incorporation seems interesting since this would result in a C:C mismatch, i.e. due to the presence of a C in the template strand (Figure 1c). A possible explanation for the apparent C:C mismatch product may invoke a slippage mechanism. Template slippage has been observed during Dpo4-mediated DNA replication on repetitive DNA sequences, and results in single-base deletions.[19] Full-length extension as well as a small percentage of dGTP insertion (7%) was observed with the

Peri:O^6-BnG pair. However, these levels were low compared with those resulting from Dpo4-mediated extension on C:O^6-BnG or BIM:O^6-BnG terminal pairs. It seems the large size and shape distortion from the Peri:O^6-BnG termini impedes PLS more than C:O^6-BnG or BIM:O^6-BnG termini.

To quantitatively address the differences in the ability of Dpo4 to extend from canonical vs mismatched (probe: template) termini, steady-state kinetics were performed. Kinetic parameters, K_m and k_{cat}, were determined under enzyme-limiting conditions and time-course measurements of $n + 1$ product formation (dGTP incorporation) were performed (Supplementary Methods). The K_m for C:G or C:O^6-BnG was 9.8 and 30 μM, respectively. Catalytic efficiency was decreased 1.9-fold when Dpo4 performed extension on C:O^6-BnG termini, in comparison to the canonical C:G terminal pair (Table 1). Steady-state parameters for the 3′-base-modified Peri

Table 1. Steady-State Kinetic Parameters for dGTP Incorporation by Dpo4

(NX)	K_m (μM)	k_{cat} (min^{-1})	Δ relative efficiency to C:G[a]
C:G	9.8 ± 0.4	1.82 ± 0.03	1
C:O^6-BnG	30 ± 5.0	2.94 ± 0.29	1.9-fold less
BIM:G	3390 ± 700	0.008 ± 0.0054	79 000-fold less

[a]Describes the ratio of $(k_{cat}/K_{m,dGTP})_{C:G}/(k_{cat}/K_m)_{N:X}$; NX represents termini base pair; BIM:O^6-BnG, Peri:G, and Peri:O^6-BnG not determined due to insufficient product formation.

primer paired opposite nondamaged and damaged templates were investigated, however no product bands were observed under all conditions tested (time points up to 72 h). The K_m for BIM:G was 3390 μM. For BIM:O^6-BnG the K_m was not accurately determined (no product observed at high dGTP concentrations (20 mM) nor time points up to 23 h). Taken together, these data suggest that alterations in base pair size and shape are important factors that influence Dpo4 catalytic efficiency during O^6-BnG-PLS and invoke the following trend in PLS rates from natural to more perturbed structures: C > BIM > Peri.

Thermal melting analysis was performed to evaluate primer:template duplex stability for placing BIM or Peri opposite G or O^6-BnG. Duplexes containing a C:G or C:O^6-BnG terminal pairs had a T_m of 70 and 68 °C, respectively. There was no difference in T_m for damaged or nondamaged templates when paired with BIM or Peri in comparison to duplexes with the natural primer (Supplementary Table 2). It was anticipated that modifications at the 3′ end of the primer, whether the terminal primer:template base pairs are matched or mismatched, would impart very little change in primer:template DNA melting behavior, and the results support this assertion.

To provide further rationale of base pairing interactions between BIM:O^6-BnG and Peri:O^6-BnG, computational studies were performed on the basis of the published crystal structure of a ternary complex of Dpo4 containing a C:O^6-BnG terminal pair and an incoming dGTP (pdb code 2jef).[15] The 3′ cytosine on the primer strand was replaced with BIM or Peri, energy minimized, and visualized. A hydrogen bond was observed between the exocyclic amino group of O^6-BnG and an imidazole nitrogen of BIM (2.11 Å, Figure 3a). No hydrogen bonds were observed between O^6-BnG and Peri in the calculated structure (Figure 3b). Although suitably arranged for H-bonding, the bulky naphthalene on Peri seems to hinder
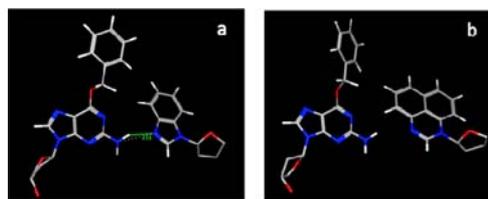

Figure 3. Modeling images of base-modified probes opposite O^6-BnG (a) BIM:O^6-BnG and (b) Peri:O^6-BnG.

a closer contact for H-bonding. The modeling results and the crystal structure lattices of BIM and Peri nucleosides reveal a striking resemblance in the hydrogen-bonding pattern (Figure S2). The crystal lattice of BIM shows an intermolecular H-bond between an imidazole nitrogen from one BIM molecule and a 5′-OH group from a neighboring BIM. In contrast, Peri utilizes two water molecules to bridge H-bonding between neighboring Peri molecules, possibly to form H-bonding without close contacts with the naphthalene moiety. These structural models suggest a potential difficulty in probing the influence of size and shape on PLS without distorting H-bonding relationships between the probe-lesion base pair. Nonetheless, these structures are useful for visualizing the size constraints within the postinsertion site.

The impact of increasing the size of alkyl groups placed in either the major or minor groove of DNA upon polymerization by Y-family polymerases has been studied previously in great detail.[20,21] However, there are no studies reported to date that investigate how bulky constituents at the primer terminus modulate extension past DNA lesions by specialized enzymes. In this study, we utilized 3′ base-modified nucleoside analogs for probing size and shape tolerances on Dpo4-mediated O^6-BnG-PLS.

Biochemical characterization of the four DNA polymerases present in *Sulfolobus solfataricus* (Dpo1−4) indicated that Dpo4 was most proficient at lesion bypass and subsequent extension.[22] In mammalian systems, DNA damage bypass can require two polymerases, i.e., one polymerase to insert and the second to extend.[23] In this context, Dpo4 has limitations in probing eukaryotic PLS. It seems DNA polymerase ζ, an "extender" polymerase in eukaryotic systems, would be a good candidate for further PLS investigation.

In the case of Dpo4-mediated PLS, the template strand has a significant role in PLS-extension fidelity. The data from the system tested in this study suggest that O^6-BnG, at the $n - 1$ position, imparts higher fidelity in comparison to the nondamaged template (at excess enzyme and dNTP concentrations relative to DNA) but that the efficiency with which the primer strand is extended seems to be strongly influenced by the base pair at the primer:template termini during PLS. The smaller BIM probe resulted in error-free and efficient $n + 1$ primer extension, when paired opposite G or O^6-BnG, in comparison to the larger Peri probe. However, relative to either BIM or Peri, the natural primer with a terminal 3′ cytosine was the most efficiently extended (dGTP incorporation) in the case of nondamaged or damaged templates.

In summary, these results implicate that (1) the size and shape of the base pair at the penultimate ($n - 1$) position during Dpo4-mediated PLS influences extension fidelity and efficiency; (2) the template strand has a strong impact on PLS fidelity; and (3) the structure of the base at the terminal position on the primer strand largely impacts extension

efficiency during PLS. Further studies are warranted using new nucleoside probes that would promote complementary adduct:probe base pairing in order to evaluate additional chemical factors (such as H-bonding) that could affect PLS.

■ ASSOCIATED CONTENT

Ⓢ Supporting Information

Experimental procedures and characterization data. Full crystallographic data has been deposited with the Cambridge Crystallographic Data Centre with deposition numbers CCDC 910347 (1) and CCDC 910348 (2). This material is available free of charge via the Internet at http://pubs.acs.org.

■ AUTHOR INFORMATION

Corresponding Author
sturlas@ethz.ch
Notes
The authors declare no competing financial interest.

■ ACKNOWLEDGMENTS

■ REFERENCES

(1) Zhang, L.; Rechkoblit, O.; Wang, L.; Patel, D. J.; Shapiro, R.; Broyde, S. *Nucleic Acids. Res.* **2006**, *34*, 3326.
(2) Gowda, P. A. S.; Krishnegowda, G.; Suo, Z.; Amin, S.; Spratt, T. E. *Chem. Res. Toxicol.* **2012**, *25*, 1195.
(3) Sale, J. E.; Lehmann, A. R.; Woodgate, R. *Nat. Rev. Mol. Cell Biol.* **2012**, *13*, 141.
(4) Berdis, A. J. *Chem. Rev.* **2009**, *109*, 2862.
(5) Merkens, L. S.; Bryan, S. K.; Moses, R. E. *Biochim. Biophys. Acta* **1995**, *1264*, 243.
(6) Fiala, K. A.; Suo, Z. *Biochemistry* **2004**, *43*, 2116.
(7) Trincao, J.; Johnson, R. E.; Wolfle, W. T.; Escalante, C. R.; Prakash, S.; Prakash, L.; Aggarwal, A. K. *Nat. Struct. Mol. Biol.* **2004**, *11*, 457.
(8) Jung, K. H.; Marx, A. *Cell. Mol. Life Sci.* **2005**, *62*, 2080.
(9) Lee, I.; Berdis, A. J. *Biochim. Biophys. Acta* **2010**, *1804*, 1064.
(10) Dahlmann, H. A.; Vaidyanathan, V. G.; Sturla, S. J. *Biochemistry* **2009**, *48*, 9347.
(11) Morales, J. C.; Kool, E. T. *J. Am. Chem. Soc.* **1999**, *121*, 2323.
(12) Yoo, J. S. H.; Guengerich, F. P.; Yang, C. S. *Cancer Res.* **1988**, *48*, 1499.
(13) Peterson, L. A. *Chem. Res. Toxicol.* **1997**, *10*, 19.
(14) Pauly, G. T.; Moschel, R. C. *Chem. Res. Toxicol.* **2001**, *14*, 894.
(15) Eoff, R. L.; Angel, K. C.; Egli, M.; Guengerich, F. P. *J. Biol. Chem.* **2007**, *282*, 13573.
(16) Maxwell, B. A.; Xu, C.; Suo, Z. *J. Biol. Chem.* **2012**, *287*, 13040.
(17) McCulloch, S. D.; Kokoska, R. J.; Masutani, C.; Iwai, S.; Hanaoka, F.; Kunkel, T. A. *Nature* **2004**, *428*, 97.
(18) Gong, J.; Sturla, S. J. *J. Am. Chem. Soc.* **2007**, *129*, 4882.
(19) Wu, Y.; Wilson, R. C.; Pata, J. D. *J. Bacteriol.* **2011**, *193*, 2630.
(20) Choi, J. Y.; Guengerich, F. P. *J. Biol. Chem.* **2008**, *283*, 23654.
(21) Maddukuri, L.; Eoff, R. L.; Choi, J. Y.; Rizzo, C. J.; Guengerich, F. P.; Marnett, L. J. *Biochemistry* **2010**, *49*, 8415.
(22) Choi, J. Y.; Eoff, R. L.; Pence, M. G.; Wang, J.; Martin, M. V.; Kim, E. J.; Folkmann, L. M.; Guengerich, F. P. *J. Biol. Chem.* **2011**, *286*, 31180.
(23) Livneh, Z.; Ziv, O.; Shachar, S. *Cell Cycle* **2010**, *9*, 729.